

# Photon-Counting Imaging with Multi-Bit Quanta Image Sensor

Jiaju Ma, Yu-Wing Chung, Abhiram Gnanasambandam, Stanley H. Chan, Saleh Masoodian  
 Gigajot Technology Inc., Pasadena, CA 91107, USA  
 jiaju.ma@gigajot.tech

## I. Introduction

Quanta Image Sensor (QIS) provides system-on-chip solutions for a wide range of consumer, scientific, and industrial imaging applications, by utilizing advanced CMOS fabrication technologies [1]. In this paper, the characteristics of the multi-bit QIS are explained, and its excellent low-light imaging capabilities under photon-limited exposure conditions with less than 2 photoelectrons/jot/frame are experimentally demonstrated at room temperature using a Gigajot QIS prototype camera (Figure 1).

## II. Multi-Bit QIS

A QIS is composed of a specialized type of pixel, called a “jot,” which provides single-photon sensitivity and accurate photon-number-resolving capability without the use of electron avalanche multiplication or cooling. By taking advantage of the photon-number-resolving capability of the demonstrated jot devices, multi-bit QIS can further extend the photon flux capacity, dynamic range, and signal-to-noise ratio (SNR), compared to the single-bit QIS and other single-photon imaging devices [2]–[4].

Different than the conventional CMOS image sensors (CIS), QIS images are constructed using spatially and temporally oversampling (Figure 1). The large array of jots in a multi-bit QIS capture the photoelectrons and output multi-bit digital signals that reflect their captured number of photoelectrons in one frame. For example, a 3-bit QIS jot can linearly resolve the number of

photoelectrons from 0 to 7 in one readout. By binning the jot outputs both spatially and temporally, high-dynamic-range image pixels can be created. If we define the spatial oversampling factor as  $S$  and the temporal oversampling factor as  $T$ , the total oversampling factor  $M$  is given by  $M = S \cdot T$ . For example,  $M$  is 64 in a 4x4x4 oversampling mechanism. The oversampling factor and the bit depth of the QIS determine the effective *FWC* of the constructed image pixels. For example, with  $M=64$  and 8-bit jots, the *FWC* equals to  $16320e^-$  ( $255e^- \times 64$ ). Different oversampling factor can be applied to the same QIS device to get different pixel sizes, spatial resolutions, and frame rates. Since the image construction process occurs post-capture, the oversampling factor can be adjusted based on the requirements of the application. Hence, it is possible for one generic QIS platform device to suffice the requirements of a wide-span of applications. By adjusting dynamically, the additional programmability also enables computational imaging/sensing capabilities in applications such as machine vision, light communication, AR/VR, and security.

## III. Demonstration of Photon-Counting Imaging

The performance of the Gigajot QIS camera module is summarized in Table 1. Additionally, a quantum efficiency (QE) curve is shown in Figure 6. The analog outputs produced by the QIS device are converted to digital signals by 14-bit off-chip ADCs. To demonstrate the behaviors of a multi-bit QIS, the digital signals are further quantized to electron numbers with different bit

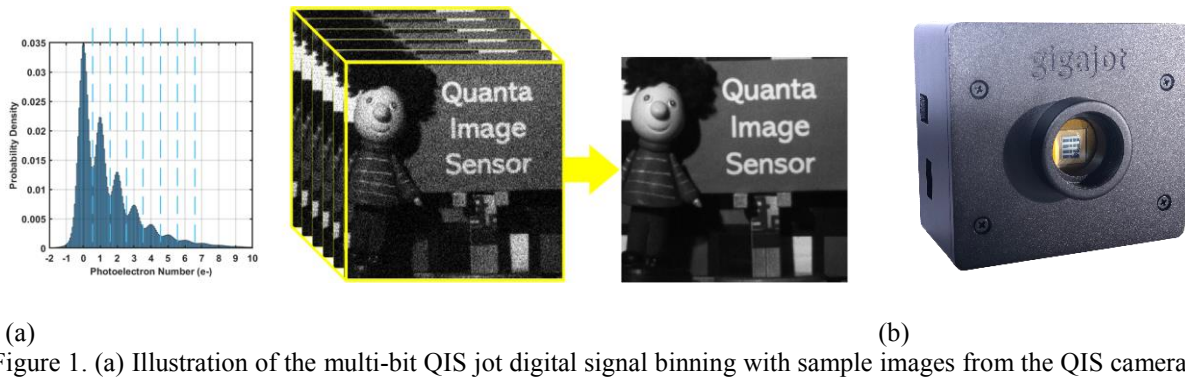


Figure 1. (a) Illustration of the multi-bit QIS jot digital signal binning with sample images from the QIS camera. The photon counting histogram of one frame is shown. (b) Gigajot QIS prototype camera module.

depths. Eventually, the photon-counting data in jot cubicles is binned spatially and temporally to create the final image pixels.

Photon-counting imaging with multi-bit QIS requires deep sub-electron read noise. The QIS jot devices used in this demonstration are implemented in a standard CMOS image sensor active pixel architecture. With multiple capacitance reduction innovations implemented the in-pixel floating diffusion node [6], [7], the conversion gain of the jot devices is improved to more than  $350\mu\text{V/e-}$  without the use of electron multiplication gain, which significantly reduces the input-referred read noise to less than  $0.25\text{e- rms}$  and enables the photon-counting capabilities under room temperature operation.

For photon-counting imaging under extremely-low illumination levels, the average photon counts from the sensor should match the quanta exposure, which is defined as the average number of photoelectrons captured by one jot in one integration period. However, false counts generated by read noise in the quantization process introduces noticeable non-linearity to the photon response characteristics when the quanta exposure is below  $1\text{e-}$  [8]. As shown in Figure 2, this non-linearity increases with higher read noise levels. The measured average response of the 1Mjot QIS matches the theoretical curve with an average  $0.25\text{e- rms}$  read noise at room temperature. There is a distribution of read noise across the jots ranging from as low as  $0.18\text{e- rms}$  with an average value of  $0.25\text{e- rms}$  as measured independently. When the photon-counting signals are constructed into images with a high oversampling factor (e.g. 10,000), this non-linearity artifact is shown in the final images as a loss of contrast (Figure 3), while under sparse-light illumination levels, higher read noise leads to a reduced SNR (Figure 4).

The noise encountered by a multi-bit QIS includes photon shot noise and read noise. With quanta exposure below  $1\text{e-}$ , the total noise is dominated by the read noise. As shown in Figure 5(a), the simulation results suggest that a reduction of read noise from  $1.00\text{e- rms}$  to  $0.15\text{e- rms}$  can effectively reduce the minimum oversampling factor required to reach  $\text{SNR}=1$  by one to two orders of magnitude, which is essential for high-speed and high-resolution low-light imaging applications. As shown in Figure 5(b), the measured SNR curves with different bit depths and oversampling factor match the theoretical models (solid lines) with  $0.25\text{e- rms}$  read noise at room temperature.

The sample images from the multi-bit QIS camera are shown in Figure 6. Three sets of images with extremely-low illumination levels less than  $2$  photoelectrons/jot/frame are presented. The SNR of the

final images can be further improved with a denoising algorithm developed for multi-bit QIS devices [9], as shown in the results in the last column of Figure 6. Combined with the denoising algorithm, a high-quality image can be produced with as low as  $12$  photoelectrons/pixel. Additionally, the SNR for even lower photon counts may already suffice the requirements for some machine vision imaging applications.

#### IV. Summary

In this paper, the Gigajot's 1Mjot Quanta Image Sensor camera module was used to demonstrate excellent low-light imaging capabilities under sparse-light illumination conditions with as low as less than  $2$  photoelectrons/jot/frame. The response characteristics of the multi-bit QIS was also measured and reported.

#### V. Acknowledgement

The quanta image sensor used in the Gigajot QIS camera module in this paper was designed by former PhD candidates, S. Masoodian, J. Ma and D. Starkey at Dartmouth Advanced Image Sensor Lab led by E. Fossum, and fabricated by Taiwan Semiconductor Manufacturing Company (TSMC) in 2016. The development of the camera system and characterization work were partially sponsored by National Science Foundation (NSF) Small Business Innovative Research (SBIR) program and NASA SBIR program.

#### References

- [1] E. R. Fossum, J. Ma, S. Masoodian, L. Anzagira, and R. Zizza, "The Quanta Image Sensor: Every Photon Counts," *Sensors*, vol. 16, no. 8, p. 1260, Aug. 2016.
- [2] J. Hynecek, "Impactron-a new solid state image intensifier," *IEEE Trans. Electron Devices*, vol. 48, no. 10, pp. 2238–2241, 2001.
- [3] N. A. W. Dutton *et al.*, "A SPAD-based QVGA image sensor for single-photon counting and quanta imaging," *IEEE Trans. Electron Devices*, vol. 63, no. 1, pp. 189–196, 2016.
- [4] I. Gyongy, N. Dutton, and R. Henderson, "Single-Photon Tracking for High-Speed Vision," *Sensors*, vol. 18, no. 2, p. 323, Jan. 2018.
- [5] J. Ma, S. Masoodian, D. A. Starkey, and E. R. Fossum, "Photon-number-resolving megapixel image sensor at room temperature without avalanche gain," *Optica*, vol. 4, no. 12, p. 1474, Dec. 2017.
- [6] J. Ma and E. R. Fossum, "Quanta Image Sensor Jot With Sub  $0.3\text{e- r.m.s.}$  Read Noise and Photon Counting Capability," *IEEE Electron Device Lett.*, vol. 36, no. 9, pp. 926–928, Sep. 2015.
- [7] J. Ma and E. R. Fossum, "A Pump-Gate Jot Device With High Conversion Gain for a Quanta Image

Sensor," *IEEE J. Electron Devices Soc.*, vol. 3, no. 2, pp. 73–77, Mar. 2015.

[8] E. R. Fossum, "Modeling the Performance of Single-Bit and Multi-Bit Quanta Image Sensors," *IEEE J. Electron Devices Soc.*, vol. 1, no. 9, pp. 166–174, Sep. 2013.

[9] S. H. Chan, O. A. Elgendi, and X. Wang, "Images from Bits: Non-Iterative Image Reconstruction for Quanta Image Sensors," *Sensors*, vol. 16, no. 11, p. 1961, 2016.

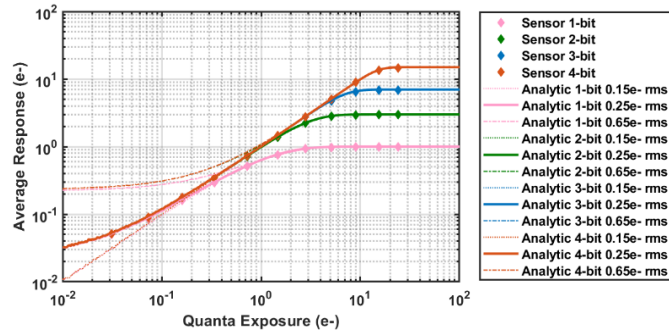


Figure 2: Photon average response curves of the 1Mpix QIS versus the analytic model.



Figure 1: Simulated images for a 2-bit QIS with different read noise (Un) levels. The quanta exposure  $H=0.3e^-$  and the oversampling factor  $M=10,000$ , equivalent to 3,000 photons/pixel in average.



Figure 4: Simulated images for a 2-bit QIS with different read noise (Un) levels. The quanta exposure  $H=0.1e^-$  and the oversampling factor  $M=1,000$ , equivalent to 100 photons/pixel in average.

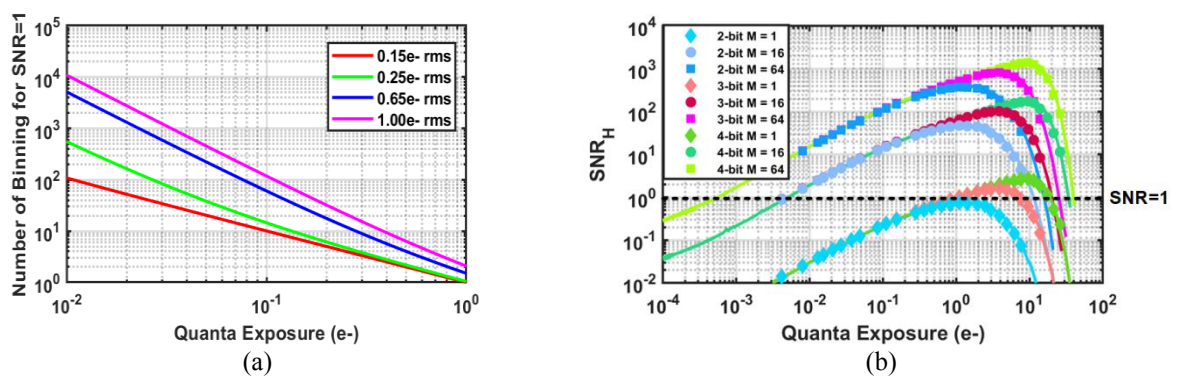


Figure 5: (a) The oversampling factor required to reach  $\text{SNR}=1$  with different quanta exposures and read noise levels. (b) Measured  $\text{SNR}_H$  curves with different quanta exposure levels, oversampling factors, and QIS bit depths.

| Specification                    | Value                |
|----------------------------------|----------------------|
| Resolution                       | 1024x1024            |
| Jot Pitch Size                   | 1.1 $\mu$ m          |
| Average Conversion Gain          | 350eV/e-             |
| Average Read Noise (27C ambient) | 0.25e- rms           |
| Linear Full-Well Capacity        | $\sim$ 80e-          |
| Peak QE                          | 86% at 480nm         |
| Dark Current (20C)               | 0.068e-/sec/jot      |
| Data Format                      | Off-chip 14-bit ADCs |
| Frame Rate                       | Up to 10fps          |

Table 1: Performance summary of the QIS pathfinder camera.

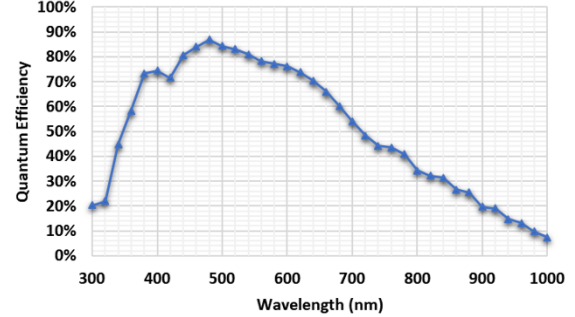


Figure 6. The quantum efficiency curve of the QIS.

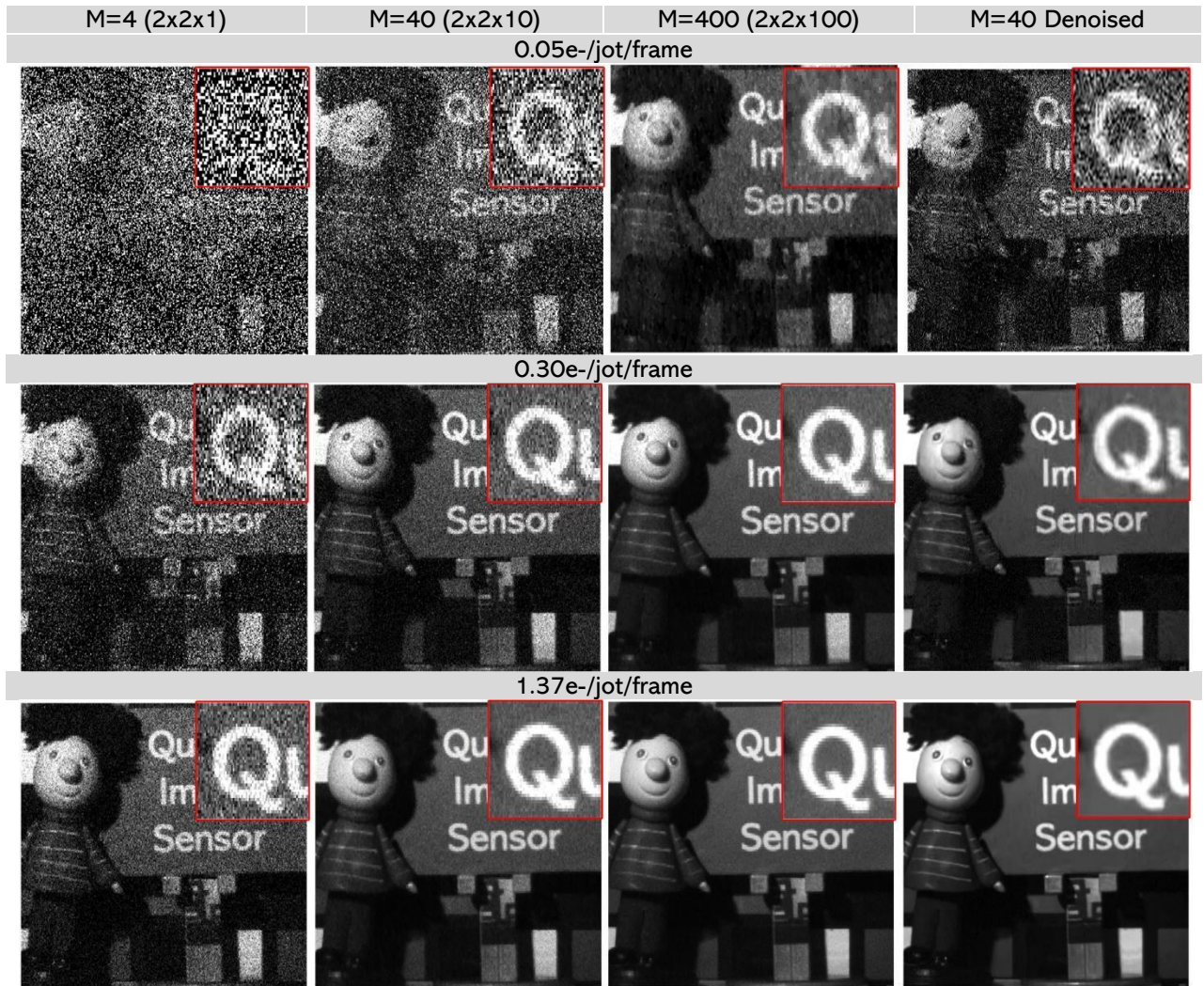


Figure 7: Sample images from the QIS pathfinder camera with 3-bit photon-counting signals and different illumination levels. The jots are binned in the digital domain with different cubicle size to create the final images. In the last column, the QIS denoising algorithm developed at Purdue is applied to the images to further improve the SNR.